Proceedings of the
8th Graz Brain-Computer Interface Conference 2019 DOI: 10.3217/978-3-85125-682-6-54

PARTIAL BRAIN MODEL FOR REAL-TIME CLASSIFICATION OF RGB VISUAL STIMULI: A BRAIN MAPPING APPROACH TO BCI

A.F. Soler-Guevara[1], E. Giraldo[2], and M. Molinas[1]

[1]Norwegian University of Science and Technology, Trondheim, Norway
[2]Universidad Tecnológica de Pereira, Pereira, Colombia

E-mail: andres.f.soler.guevara@ntnu.no

ABSTRACT: Brain-computer interface (BCI) applications are characterized by real-time feature extraction and classification. Thus, brain activity reconstruction is not generally performed due to the long computation times required to estimate brain activity. Here, we present a method for applying brain mapping solutions to BCI applications, based on a reduced model of the brain covering the occipital region using only four local electrodes (P3, P4, O1, and O2) for the classification of red, green, and blue (RGB) visual stimuli. We obtained a classification accuracy of 100% within feasible estimation times for BCI applications using an event-related potential (ERP) dataset. We first validated the occipital-zone model with a test using synthetic EEG data to evaluate its performance for local brain mapping with a small number of electrodes. In a second test, we used the validated partial model to map the occipital and part of the parietal lobes for RGB classification with outstanding results.

INTRODUCTION

Brain-computer interface systems (BCI) use brain activity to control external devices, improving the capacity of the interaction of people with disabilities or allowing a user to generate a command to actuate a device directly from the brain. BCI systems based on electroencephalograms (EEGs), use the electrical signals from electrodes in the scalp as a non-invasive technique to obtain neural activity information corresponding to human activity or external stimuli. Then, a feature extraction process from the data allows the classification of several human activities to generate a command that can actuate devices. Thus, the time between data acquisition and generation of the command is critical for developing real-time applications. The brain-mapping approach has not been considered for BCI applications due to the computational time required to process large head models and estimate a solution.

Brain mapping solutions provide an estimation of the cortical activity from the information measured with electrodes in the scalp. Such an estimation is known as the inverse problem solution from EEG. It has, however, the characteristics of being ill-posed and ill-conditioned, due to the reduced number of electrodes (hundreds), limited available information, and the high quantity of points of activity or distributed sources (thousands) to be estimated. Several methods have been presented in the literature to overcome such conditions, but brain mapping is a time-consuming technique and the quality of the solutions is highly dependent on the number of electrodes. Thus, BCI systems are rare and have not been widely studied. However, in [1] the authors present a simplified EEG inverse solution through the use of a small quantity of dipoles in the Broadmann areas, where the dimension of the inverse problem is reduced, opening the possibility to use this type of representation in BCI systems due to the reduced computational time. In [2] the feasibility of combining the source of information and electrode information was studied using a right-hand imaginary task. This study paved the way to the possibility of improving BCI solutions with brain mapping. However, in both studies, a full-brain model was considered and the solutions were not focused on specific areas of the brain, as we are proposing.

Here, we investigated a method for estimating brain activity using a partial brain model, based on a specific zone of the brain, the occipital zone and part of the parietal region, and fewer electrodes around this zone. Moreover, we present a BCI application for classifying RGB colors, obtaining a remarkable improvement over the classification results shown in [3], using the same database for classifying the three colors in real-time. This method paves the way for online BCI applications involving brain mapping techniques.

MATERIALS AND METHODS

EEG Forward model:

The equation which relates the signals measured in the scalp with the activity inside the brain is known as the EEG forward equation, and can be represented as shown below in 1

$$y_k = Mx_k + \varepsilon_k \tag{1}$$

with $\boldsymbol{y}_k \in \mathbb{R}^{d \times N}$ being the observed EEG measurements and containing the signals of d electrodes and N the total

 DOI: 10.3217/978-3-85125-682-6-54

number of samples, where the subscript k is the sample associated with the time instant $t_k = kh$ which represents the $k-$th sample of the EEG recording, where $k = 1, ..., N$ and h the sample time. The term $x_k \in \mathbb{R}^{n \times N}$ represents the source activity inside the brain that produces the measured electrical impulses. In a head model based on distributed sources, n is the number of sources considered in the brain. The matrix $M \in \mathbb{R}^{d \times n}$ is the lead field matrix or sensor matrix, which relates the measured EEG y_k to the neural activity x_k; and represents the current flow from each source to each electrode. In addition, white noise is considered in the measurements and is represented by ε_k with a mean of zero and C_ε covariance.

EEG Inverse problem solutions:
The EEG inverse problem has several characteristics that are difficult to manage -the neural activity reconstruction is an ill-conditioned and ill-posed problem- where the solution is highly noise dependent and an infinite number of estimations of the activity $\hat{x}_k$ can explain the same measurement in the EEG y_k. These issues can be overcome by several potential solutions found in the state-of-the-art, based on constrained minimum norm regularization, such as minimum norm estimation (MNE) [4], low-resolution tomography (LORETA) [5] and and the iterative regularization algorithm based on the L2 norm (IRA L2) [6],and probabilistic frameworks, such as the dynamic multi-model source localization method (DYNAMO) [7] and multiple sparse priors (MSP) [8]. We selected two methods to estimate the underlying neural activity, MSP and IRA L2, of which the approaches are briefly presented below. The MSP method assumes a priori that the activity x_k follows a normal distribution with zero mean and covariance C_x. Based on this assumption, the expected operator is applied to estimate the activity.

$$\hat{x}_k = E[p(x_k|y_k)] \tag{2}$$

After applying the Bayes theorem and further mathematical manipulations, the estimation is performed by:

$$\hat{x}_k = C_x M^T (C_\varepsilon + M C_x M^T)^{-1} y_k \tag{3}$$

where the problem is centered on estimating the covariance matrices C_ε and C_x. On the other hand, the IRA L2 method is based on a constrained minimum norm solution adding spatial and temporal constraints, such as the following cost function:

$$J = ||Mx_k - y_k||_2^2 + \rho_k^2 ||x_k||_2^2 + \lambda_k^2 ||x_k - x_{k-1}||_2^2 \tag{4}$$

where the solution involves the temporal behavior of the sources and their location, involving the terms ρ_k and λ_k, which are the regularization parameters related to the spatial distribution of the sources and the temporal evolution of the activity. The estimation can be performed using the equation below:

$$\hat{x}_k = (M^T M + \rho_k^2 I + \lambda_k^2 I)^{-1} (M^T y_k + \lambda_k^2 x_{k-1}) \tag{5}$$

Zone-Based Partial Brain Model:
The lead field matrix M represents the current flow from each of n sources to each of d electrodes. This matrix usually involves the conductivity of the skull, skin and grey matter as in [9], which is obtained to relate the neural activity x_k to the measurements in the scalp y_k as well as possible. The formation of the matrix is developed by numerical methods, such as the finite element method (FEM) and the head model considers the position of the electrodes and establishes the position of the distributed sources. For the proposed zone-based partial brain model, the model for a specific zone is created by applying a spatial filter for evaluating which sources belong to the target zone. Then, the columns corresponding to the sources in the target zone are selected from the gain matrix M and appended in a new temporal matrix $M_{rs} \in \mathbb{R}^{d \times rs}$, with rs being the number of reduced sources. At this point of the reduction, we work under the first assumption that *all the measured activity in the electrodes can be found in the target zone*, an assumption that is not true, because the activity can be generated in another zone of the brain and projected in the target zone. However, a second assumption is considered, in which *the activity registered in an electrode mostly represents activity in the neighbor spaces around it*. Under this assumption, the rows corresponding to the nearest electrodes in the zone can be selected from the matrix M_{rs}, and appended to form a lead field matrix of the target zone $M_{rz} \in \mathbb{R}^{rd \times rs}$ with rd being the number of reduced electrodes. This assumption reduces the effects of the first and allows us to create a hypothesis in which *the activity in a reduced zone, can be mapped with a reduced number of electrodes around such a zone*. Here, the forward reduced problem can be represented by the following equation:

$$y_{rz_k} = M_{rz} x_{rz_k} + \varepsilon_k \tag{6}$$

where y_{rz_k} represents the measurements in the reduced set of electrodes and x_{rz_k} the activity in the sources that belong to the target zone.

EXPERIMENTAL SETUP

We performed two experiments to evaluate the presented hypothesis and explore the use of the zone-based partial model in a BCI application. We used a database presented and used in [3] for RGB color classification, which contains the information of the electrodes P3, P4, O1, and O2. The tests are described below:

Test 1: Mapping the Occipital region:
We evaluate the hypothesis by simulating the activity of one random source in the aforementioned region and calculating the EEG with 60 electrodes (Fpz, AF7, AF3, AFz, AF4, AF8, F7, F5, F3, F1, Fz, F2, F4, F6, F8,

 DOI: 10.3217/978-3-85125-682-6-54

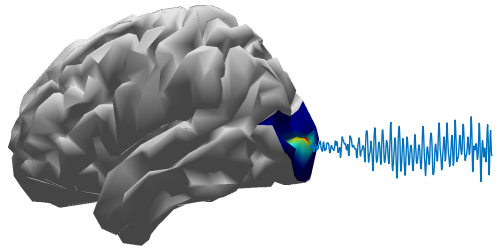

Figure 1: Simulated activity in the occipital region using the full brain model.

FT7, FC5, FC3, FC1, FCz, FC2, FC4, FC6, FT8, T7, C5, C3, C1, Cz, C2, C4, C6, T8, TP7, CP5, CP3, CP1, CPz, CP2, CP4, CP6, TP8, P7, P5, P3, P1, Pz, P2, P4, P6, P8, PO7, PO3, POz, PO4, PO8, O1, Oz, O2, and Iz) according to the standard 10-10 layout, using equation 1 involving the standard head model presented in [9], in which a mean head model from a 152 participant MRI study was computed using the FEM method, considering the position of 231 electrodes. The zone model was computed for the occipital and part of the parietal regions. Fig.1 shows an example of simulated activity in the target zone using the full brain forward equation. The simulated activity corresponds to normal activity based on a continuum brain model of the neuronal activity presented in [10], which was used in [6] and [11] performing a sampling using the model in Eq.7, in which the activity is represented in discrete time.

$$\frac{1}{\gamma^2}\frac{d^2\boldsymbol{x}(t)}{dt^2}+\frac{2}{\gamma}\frac{d\boldsymbol{x}(t)}{dt}=c_1\boldsymbol{x}(t)+c_2\boldsymbol{x}(t-t_0)+c_3\boldsymbol{x}^2(t)+c_4\boldsymbol{x}^3(t)+\eta \tag{7}$$

where the constants C_i with $i = 1,2,3,4$ represent the instantaneous feedback due to nearby neurons and delayed feedback via an extra-cortical loop, t_0 is a time delay, and γ is a characteristic decay rate of the field activity $\boldsymbol{x}(t)$. η is random white noise and considered to be an external stimulus that perturbs the brain states. With the activity x_k equation 1 was computed to obtain an EEG. Then, noise was added in the electrodes using a signal-noise-ratio (SNR) of 50db, after which, the brain mapping was performed in two ways: the first, using the full head model with 2000 distributed sources and 60 electrodes, and the second, using the set with the occipital model with 622 distributed sources, and the P3, P4, O1, and O2 electrodes as the EEG dataset in [3]. In both cases, the MSP and IRA L2 methods were applied to estimate neural activity. The overall process followed is summarized in the Fig.2

Five thousand trials of random activity were generated. The error measurements to evaluate the performance of the algorithms with the zone-based partial brain model and full brain model were: the localization error of the estimated source and the relative error between the simulated and estimated activity, using the following expressions:

$$RelE = \frac{||\hat{x}_k - x_k||_2^2}{||x_k||_2^2} \tag{8}$$

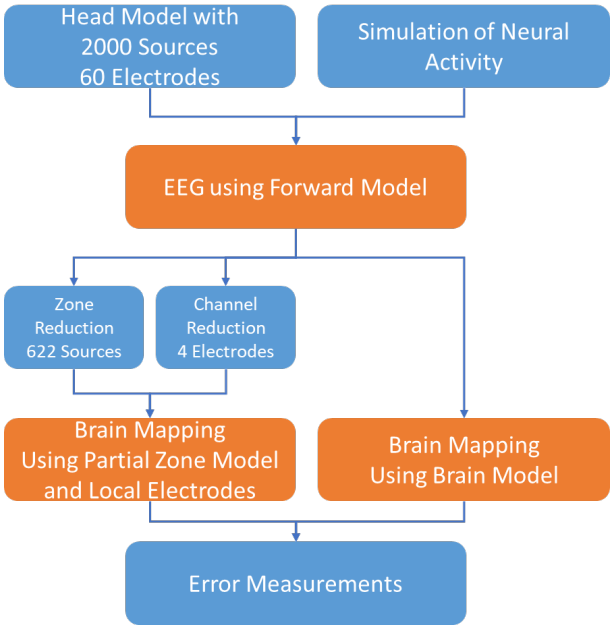

Figure 2: Test 1: Flowchart explaining the zone-based partial brain model and its validation procedure.

$$LocE = ||\hat{P}_x - P_{\hat{x}}||_2 \tag{9}$$

where P_x represents the 3D position in a coordinated space of the simulated activity and $P_{\hat{x}}$ the position of the maximum amplitude source in the estimated activity.

Test 2: RGB ERP classification using the occipital region-based partial brain model:

A dataset of seven subjects exposed to red, green, and blue visual stimuli was used in this experiment, as presented in [3]. The event-related potentials (ERP) were taken with a g.tec g.MOBIlab+ portable device sampled at 256 Hz, for which each color was randomly presented 60 times, resulting in 60 trials of each color for each subject. These data were used to perform brain mapping using an occipital lobe and part of parietal lobe partial brain model with 622 distributed sources, involving the four aforementioned electrodes. The inverse solutions were performed using the MSP and IRA L2 methods to obtain the source space. The mapped source space was divided into 64 and 81 sub-regions, using the mean of the sources involved in each one of the sub-regions as features for classification. The data were normalized and then classified using the naive Bayes and decision tree classifiers techniques with 10-fold cross-validation.

The procedure followed for the test, feature extraction and classification of the activity are summarized in Fig. 3 and how the division was performed for the 81 features is depicted in Fig. 4 depicts . As shown in the images, there were no sources involved in the upper corners. Thus, these features were removed and not considered for the classification process.

An evaluation of computational time performing brain mapping, feature extraction, and classification are part of

 DOI: 10.3217/978-3-85125-682-6-54

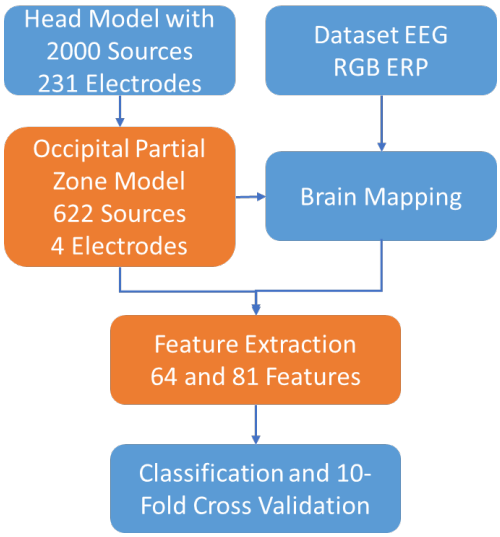

Figure 3: Test 2: Flowchart explaining the RGB ERP classification procedure.

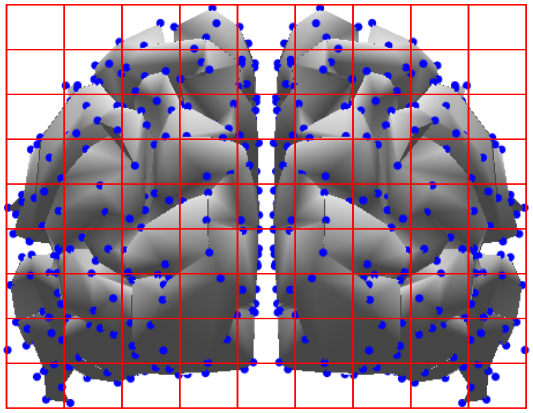

Figure 4: Occipital Zone division for feature extraction.

the study. To measure the execution times and run the algorithms, a computer with the following characteristics was used: 16GB RAM, Core i7-4790 processor, OS windows 10 64-bit, and Matlab® 2016b.

RESULTS AND DISCUSSION

Test 1 Results: The results from the first test are shown in Figs. 5, 6 and 7, in which the Fig. 5 shows the mean of the localization error and the relative error, measured between the simulated and estimated sources with the two applied methods for the reconstruction with 60 electrodes using the full brain model and four electrodes using the occipital model. As expected, the localization errors were higher if the zone model was used. The the error using the zone model was approximately 23mm, whereas the mean separation between was approximately 13 mm. This can be explained by the loss of information due to the reduction in the number of electrodes.

The localization error can be reduced by increasing the number of sources in the brain model. Nonetheless, the activity was clearly identifiable in all the cases (6).

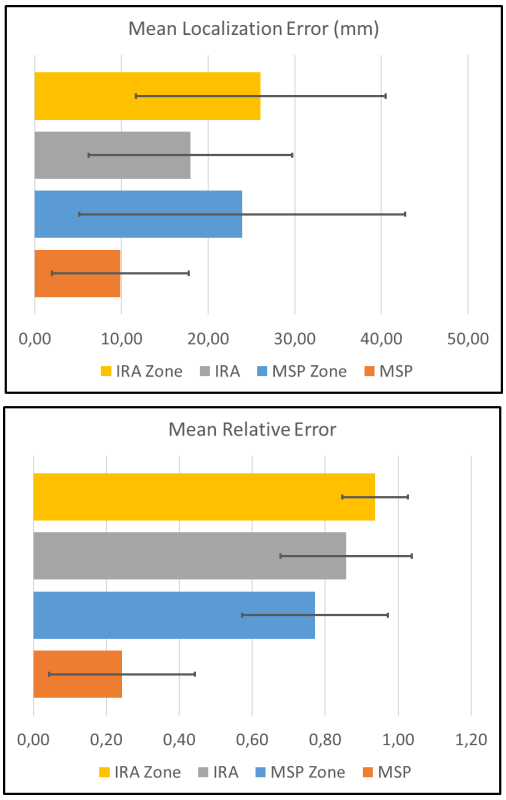

Figure 5: Mean localization error (Top) and mean relative rrror (Bottom) across the 5000 trials with the proposed zone-based partial brain model and MSP and IRA L2 methods.

MSP with the full brain model achieved the lowest relative error, because MSP gives the best results in experiments with one source estimation, as explained in [12]. However, the partial model with MSP obtained a lower error value than IRA L2 method with the full brain model. In addition, the activity with the partial and full brain models showed a highly similar pattern, with similar amplitude, using MSP (Fig. 7). The activity with IRA L2 showed a simmilar pattern but the amplitude was attenuated, explainning why the relative error with IRA L2 was higher in the two cases (Fig. 7).

A reconstruction between the simulated activity and the solutions with the full brain and partial occipital brain model for visual comparison, performed with the MSP method, showed the simulated and reconstructed activity to be highly similar with a only small error in source localization (Fig. 6). The simulated activity and each of the reconstructions results obtained using MSP and IRA L2 are shown in Fig. 7. The MSP reconstruction with the brain model overlapped the simulated activity. The other reconstructions followed a pattern similar to the original, with the MSP reconstruction using the zone model showing a smaller difderence in amplitude than for the other reconstructions.

The differences in amplitude between IRA L2 reconstruction and the simulated source can be explained by the fact that the IRA L2 solutions are smooth, which means that the source amplitude of the true source is represented by a combination of amplitudes of several

 DOI: 10.3217/978-3-85125-682-6-54

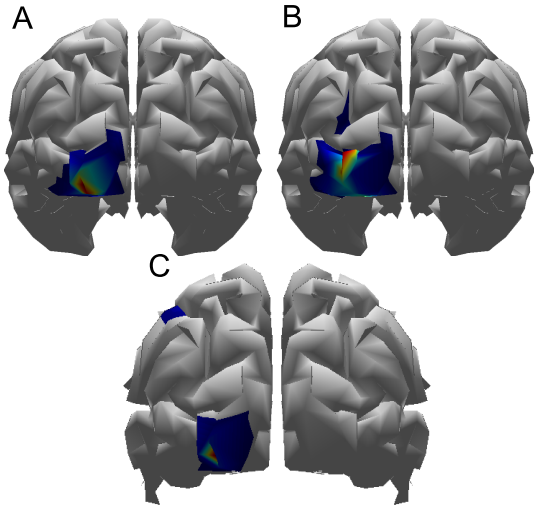

Figure 6: Simulated activity (A), estimated activity using the full brain model with MSP (B) and estimated activity using the zone model with MSP (C).

neighbors sources in the reconstruction and the source with the maximum mean activity in time is used for calculating the relative error.

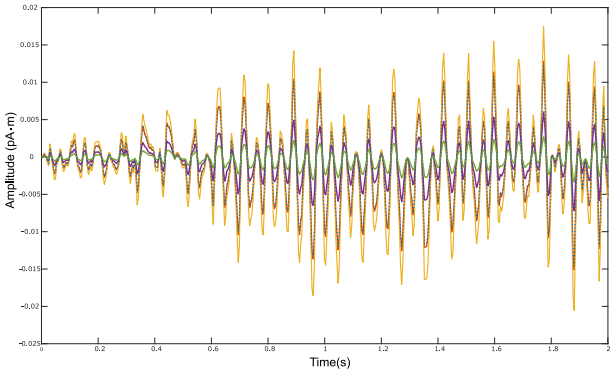

Figure 7: Simulated activity (blue dots), MSP (orange) and IRA L2 (purple) reconstructions using the full brain model and MSP (yellow) and IRA L2 (green) reconstruction using the zone model.

Test 2: RGB Classification Results: The classification results of the second test are summarized in 1, in which the naive Bayes classifier achieved and accuracy of 99.6% and 100% with 64 and 81 features, respectively. The decision tree classifier achieved a 100% for both number of features. These results shown that each of the RGB colors can be uniquely represented as a combination of activity in terms of localization and intensity as shown in Fig. 8 in which the mean of the 64 features for the seven subjects and 420 trials is presented for each color.

Table 1: Classification accuracy with the two classifiers, and feature numbers for RGB visual stimuli.

Feature Numbers	Naive Bayes	Decision Tree
64	99,6% ± 0,3	100% ± 0
81	100% ± 0	100% ± 0

The computational time for brain mapping, feature extraction, and classification using the two inverse solutions for a three-second window of the trial is shown in Table 2. In summary, a solution that includes the aforementioned steps can be performed in approximately 150 ms for the longest combination, using MSP for brain mapping and naive Bayes for classification, and 45 ms for the shortest combination, using IRA L2 and the decision-tree for classification. These results show that the methodology proposed here is feasible for BCI implementation and general online applications.

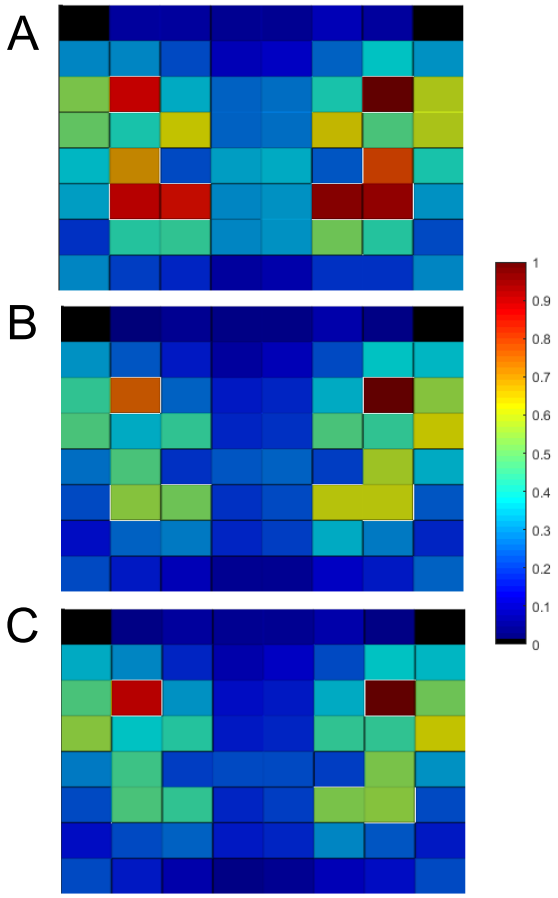

Figure 8: Mean of 64 features for the seven subjects for red (A), green (B) and blue (C).

Table 2: Computational times for brain mapping, feature extraction, and classification steps in the RGB classification.

	Time (ms)	
Process /Methods	MSP zone	IRA L2 zone
Brain Mapping	101,8 ±5,2	27,3 ±3,2
Feature Extraction	12,1 ±0,2	
Naive Bayes Classification	35,1 ±0,2	
Decision Tree Classification	4,9 ±0,1	

CONCLUSIONS AND FUTURE WORK

We performed experiments with the zone-based partial brain model methodology using synthetic EEG and visual ERP. We studied the behavior of the estimations using a reduced number of local electrodes. Based on the

 DOI: 10.3217/978-3-85125-682-6-54

accuracy of the results presented herein, activity can be mapped using a zone-model and electrodes around this area for the given stimuli.

Our classification results showed high accuracy in relatively short computational times, suitable for BCI applications. These encouraging results show promise for the extension of the same methodology to other brain zones, depending on the neuro-paradigm studied. Some immediate applications could be the classification of motor cortex activity in motor or imaginary motor tasks, diverse visual and auditory stimuli, and emotions.

The signature of the RGB colors can be represented as a combination of intensities of activities in the sources located around the visual cortex in the occipital lobe. This test can be extended for the evaluation of more colors and their differentiation in the cortical space.

The next step in this research will be the experimental demonstration of the uniqueness of the RGB signatures in device actuation. An ON/OFF actuation command will be sent to actuate a device using the signatures obtained from RGB stimuli on-line with the proposed method. The partial brain model approach will be further evaluated for various neural activities to assess the real-time capabilities of the method for a wider set of human activities and external stimuli.

ACKNOWLEDGMENTS

This work was funded by the Norwegian University of Science and Technology NTNU project "David and Goliath: single-channel EEG unravels its power through adaptive signal analysis" where a concept of FlexEEG is being developed for scanning the activity inside the brain with a reduced number of electrodes using a moving robotic headset over the scalp.

REFERENCES

[1] Duque-Muñoz L., Vargas F., López J. D. Simplified EEG inverse solution for BCI real-time implementation. In: 2016 38th Annual International Conference of the IEEE Engineering in Medicine and Biology Society (EMBC). 2016, 4051–4054.

[2] Ahn Minkyu, Hong Jun Hee, Jun Sung Chan. Feasibility of approaches combining sensor and source features in brain–computer interface. Journal of Neuroscience Methods. 2012;204(1):168 –178.

[3] Rasheed Saim, Marini Daniele. Classification of EEG Signals Produced by RGB Colour Stimuli. Journal of Biomedical Engineering and Medical Imaging. 2015;2(5):56.

[4] Hyder R, Kamel N, Tang T B, Bornot J. Brain source localization techniques: Evaluation study using simulated EEG data. 2014 IEEE Conference on Biomedical Engineering and Sciences (IECBES). 2014 (;December):942–947.

[5] Pascual-Marqui R D, Michel C.M., Lehmann D. Low resolution electromagnetic tomography: a new method for localizing electrical activity in the brain. International Journal of Psychophysiology. 1994;18(1):49–65.

[6] Giraldo-Suarez E., Martinez-Vargas J. D., Castellanos-Dominguez G. Reconstruction of Neural Activity from EEG Data Using Dynamic Spatiotemporal Constraints. International Journal of Neural Systems. 2016;26(07):1650026.

[7] Antelis Javier M., Minguez Javier. DYNAMO: Concurrent dynamic multi-model source localization method for EEG and/or MEG. Journal of Neuroscience Methods. 2013;212(1):28 –42.

[8] Friston Karl et al. Multiple sparse priors for the M/EEG inverse problem. NeuroImage. 2008;39(3):1104–1120.

[9] Huang Yu, Parra Lucas C., Haufe Stefan. The New York Head—A precise standardized volume conductor model for EEG source localization and tES targeting. NeuroImage. 2016;140:150 –162.

[10] Kim J. W., Shin H.-B., Robinson P. a. Compact continuum brain model for human electroencephalogram. Proceedings of SPIE. 2007;6802:68020T–68020T–8.

[11] Soler Andrés Felipe, Muñoz-Gutiérrez Pablo Andrés, Giraldo Eduardo. Regularized State Observers for Source Activity Estimation. In: Brain Informatics. Ed. by Wang Shouyi et al. Cham: Springer International Publishing, 2018, 195–204.

[12] Soler A. F., Giraldo E. Non-Linear Iterative Regularization Algorithm for Neural Activity Reconstruction from EEG Data. In: 2018 IEEE ANDESCON. 2018, 1–4.